J. Fluid Mech. (1989), *vol.* 201, *pp.* 189–201
Printed in Great Britain

Sideband damping of water waves over a soft bed

By MOSTAFA A. FODA
Hydraulic and Coastal Engineering, Department of Civil Engineering, University of California, Berkeley, CA 94720, USA

(Received 22 April 1988)

The Benjamin & Feir sideband instability of gravity waves over a rigid bed is extended here to the case of wave propagation over a compliant bed. The bed is assumed elastic with inhomogeneous properties, following some vertical stratification profile. The elastic stiffness at the mudline is assumed very small, as is typically the case for upper-stratum gel-like marine mud, so that its effect is assumed comparable in magnitude with that of wave nonlinearity. It is then shown that through the sideband instability, the carrier gravity wave would lose energy to sideband oscillations. These sidebands will be shown to be contaminated with small-amplitude, but very short elastic shear waves. These shear waves will interact with the viscous boundary layer at the bed–water interface, and thus significantly enhance the viscous damping of wave energy in the boundary layer.

1. Introduction

The absence of large waves is the most obvious feature of major coastal mud-bank regions around the world. Many of these mud banks are along open ocean coasts where they are frequently subjected to the full loading of storm waves coming from deep water. This is primarily attributed to the extraordinary ability of the gel-like bottom mud to dissipate the incoming water-wave energy. Examples of major open coast mud-banks include those of the southwest coast of India, the northeast coast of South America, and in the Gulf of Mexico basin. Observations from the SW Indian Coast and the Louisiana 'mud hole' indicate that the dissipative mechanism of the mud banks becomes 'fully activated' during storm conditions (e.g. Jacob & Qasim 1974; Wells 1983; Bea 1974), resulting in exceptionally high wave damping rates. For example, during the SW monsoon season, incident storm waves off Kerala, India, are observed to become almost completely damped out within a distance of only 4–8 wavelengths as they cross into the mud-bank region (MacPherson 1980). The boundaries of the mud-bank accumulations can then be mapped visually because of this rather sudden calming effect on incident waves.

Various theories have been proposed for the dissipation mechanism. Gade (1958) and Dalrymple & Liu (1978) assumed that the mud behaves as a very viscous fluid and considered the internal friction dissipation inside the mud layer as it interacts with the overlying water layer. Hsioh & Shemdin (1980) and MacPherson (1980) proposed instead a linear Voigt-body, or a viscoelastic model for the bed material. In these studies, the eigenvalue problem of the coupled seawave–seabed system was solved yielding both the dispersion relation for the surface water waves and the damping rate of these waves (the real and imaginary parts of the surface-wave eigenvalue, respectively). Although the obtained damping rates are significantly higher than those predicted by earlier rigid-bed bottom friction models (e.g. Putnam 1949), they are still too small, for realistic values of marine mud viscosities, to

explain some of the observed spectacular dampings, especially during storm wave conditions. A more serious shortcoming of these above-mentioned linear damping models is that the observed enhancement of damping during severe wave loading is a basic *nonlinear* feature of the problem that cannot be explained by a linear model.

The present paper re-examines the interaction problem between surface gravity waves and a flexible bed that is both elastic and viscous. The analysis is extended to the nonlinear domain where it will be shown that the Benjamin & Feir (1967) sideband instability of gravity waves over rigid bed applies here just as well. In the presence of the elasticity and viscosity of the bed, this instability will be shown to lead to the transfer of energy from the carrier wave to highly dissipative sideband oscillations. Thus, in our proposed damping mechanism, the energy is first lost to the sideband, which in turn loses its acquired energy to bed friction. Although energy is ultimately lost to viscous friction, it will be shown that both the elasticity and the viscosity of the mudline are playing a central role in the dissipation mechanism. In fact, the main purpose of this paper is to highlight the important role of the mudline elasticity in enhancing viscous damping.

Let us start by comparing the scales of the viscous *vs.* the elastic response in the seabed for typical marine mud properties. For bed viscosity, it can be seen from a simple dimensional argument that although mud viscosity can be as large as 10^4 times that of water or even larger (e.g. Dalrymple & Liu 1977), its effect is still small relative to the elasticity and gravity effects. This can be shown by comparing the lengthscales associated with each effect. For a wave frequency ω the gravity lengthscale k^{-1} would be g/ω^2 (k is the gravity wavenumber), while the viscous lengthscale δ would be $(\nu/\omega)^{\frac{1}{2}}$ where ν is the kinematic viscosity. On the other hand, the bed elasticity lengthscale s_0^{-1} (s_0 is the elastic shear wavenumber) is defined in terms of the bed material shear modulus G_0 and density ρ_0 as $s_0^{-1} \sim (G_0/\rho_0\,\omega^2)^{\frac{1}{2}}$. For representative values of upper-stratum marine mud properties $\nu \sim 10^{-4}$–10^{-2} m^2/s, $G_0 \sim 10^4$ kPa, and $\rho_0 \sim 10^3$ kg/m^3 (e.g. Bea 1974) we see that a typical 10 s water wave will yield a viscous lengthscale $\delta \sim 0.01$–0.1 m which is much smaller than $s_0^{-1} \sim 5$ m and $k^{-1} \sim 150$ m. This clearly suggests a boundary-layer treatment for the viscosity effects. The adopted boundary-layer structure is shown in figure 1 where the viscous behaviour is assumed to be confined within a thin interfacial layer at the mudline. The behaviour in the water above is assumed inviscid, and elastic in the bed below.

Another important observation from the above-dimensional argument is the large difference between the gravity and the elastic lengthscales. The smallness of the ratio $\mu = k/s_0$ is a manifestation of the small elasticity that characterizes the gel-like mud of many of these coastal mud-bank regions. In fact, it will be assumed here that the elasticity lengthscale is of the same order of magnitude as the wave amplitude $A \sim O(1)$ m. Thus, the relative effect of mudline elasticity is assumed comparable in magnitude with the wave's nonlinearity effect $\sim O(kA)$. With increased depth from the mudline, however, the elasticity or stiffness of the bed material will, in general, increase because of consolidation effects, resulting in some sort of a stratification profile in the seabed. In the present analysis a slow stable stratification in the bottom mud will be assumed, i.e. a slow transition from the soft condition near the mudline to a stiff bed condition far deep into the seabed. A simple WKB solution will be employed to model the response in the stratified bed. The main feature of the WKB bed solution is the presence of a turning point below which the solution is exponentially decaying to infinity.

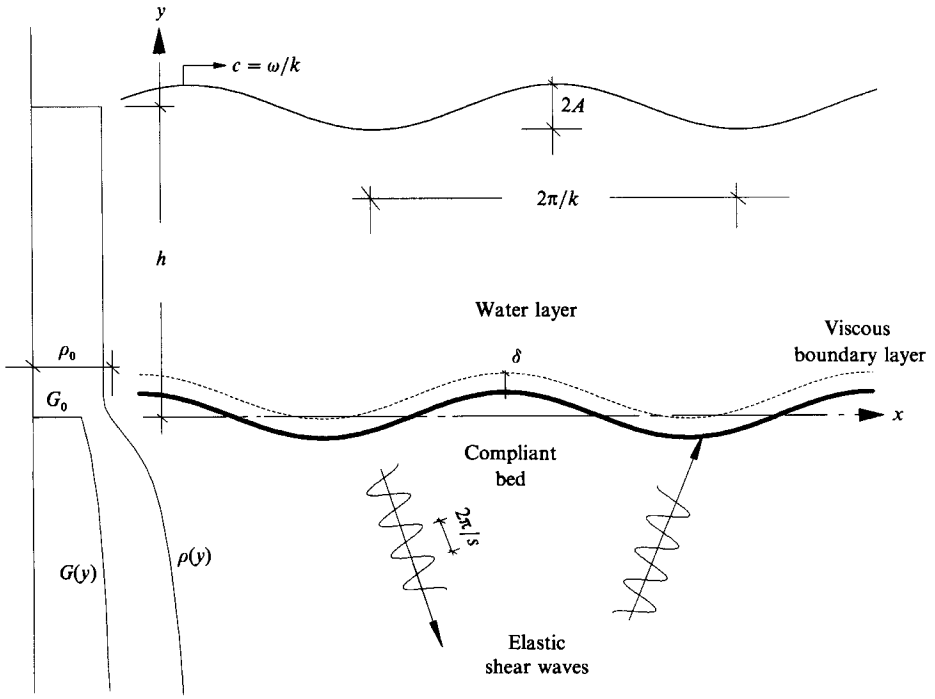

FIGURE 1. Definition sketch for the water wave–compliant bed system. Viscosity is confined to a thin boundary layer at the mudline. The small elastic response below the mudline will be in the form of a standing shear wave of very short wavelength compared to the gravity wavelength.

The analysis will show that the small mudline elasticity will give rise to a highly unstable equilibrium around the surface gravity-wave solution. The linear solution itself is shown to be largely unaffected by the mudline elasticity and viscosity. However, slightly perturbing the solution by unstable sideband modulations will enhance the viscous damping of the wave. This is primarily because these unstable sidebands are also highly dissipative wave modes. The strong damping of these sidebands is caused by the presence of standing elastic shear waves in them. These shear waves, although very small in amplitude, are also very short in wavelength and hence can have an $O(1)$ effect on the shear stress field in the bed. Therefore, such shear waves would have a significant dissipative capacity through their interaction with the viscous boundary layer at the mudline. A sideband instability analysis is worked out here to examine in some detail this proposed damping mechanism.

2. The boundary-layer formulation

Let a progressive water wave of frequency ω and wave amplitude A propagate in an inviscid water layer of depth h above an incompressible elastic bed that occupies the lower half-plane $y < 0$. The elastic modulus G of the bed material is assumed to increase gradually with depth, starting from a small value G_0 near the mudline $y = 0$. Associated with the increase in G, there is a gradual increase in the density ρ of the bed material, following some stratification profile, with $\rho = \rho_0$ at the mudline, as sketched in figure 1. Thus, the mudline elasticity is characterized by the elastic lengthscale s_0^{-1},

$$s_0^{-1} = (G_0/\rho_0\omega^2)^{\frac{1}{2}}, \tag{1}$$

where s_0 is the elastic shear-wave wavenumber at the mudline. We assume here that s_0^{-1} is of the same order of magnitude as the wave amplitude A, i.e.

$$s_0 A \sim O(1), \tag{2}$$

which simply means that the mudline elasticity effect is assumed to be of the same order of magnitude as the water-wave nonlinearity effect. In other words, if we scale both s_0^{-1} and A by the much larger water-wave lengthscale $k^{-1} = g/\omega^2$ we get

$$\mu = k/s_0 \sim O(\epsilon) \ll 1, \tag{3a}$$

where ϵ is the wave nonlinearity (wave steepness)

$$\epsilon = kA \tag{3b}$$

and μ is the measure of the mudline elasticity.

A viscous boundary layer of thickness $\delta \sim (\nu/\omega)^{\frac{1}{2}} \ll (s_0^{-1}, k^{-1})$ is fitted at the mudline in order to satisfy the conditions of continuity of shear stress and tangential velocity across the water–bed interface. The kinematic viscosity ν is taken to represent the combined viscosity of the water–mud mixture at the mudline. With these scalings we proceed with the statement of the problem.

(i) In the inviscid water layer, the horizontal and vertical velocities, u and v, are given in terms of the velocity potential Φ, i.e.

$$u = \frac{\partial \Phi}{\partial x}, \quad v = \frac{\partial \Phi}{\partial y}, \tag{4}$$

and Φ satisfies Laplace's equation

$$\nabla^2 \Phi = 0 \tag{5}$$

and the nonlinear free-surface boundary condition at $y = h$

$$\begin{aligned} \Phi_{tt} + g\Phi_y = {} & [-\tfrac{1}{2}(\nabla\Phi)^2 + \tfrac{1}{2}\Phi_t \Phi_{yt}]_t - [\Phi_x \Phi_t]_x \\ & + \frac{1}{2g^2}[g(\Phi_t(\nabla\Phi)^2)_y - 2\Phi_t \Phi_{yt}^2 - \Phi_{yyt} \Phi_t^2]_t \\ & + \frac{1}{2g}[-g\Phi_x(\nabla\Phi)^2 + 2\Phi_x \Phi_t \Phi_{yt} + \Phi_t^2 \Phi_{xy}]_x + O(\Phi^4), \quad y = h. \end{aligned} \tag{6}$$

Compared with the left-hand side, the quadratic and cubic terms on the right are of the order $O(\epsilon)$ and $O(\epsilon^2)$, respectively.

(ii) In the elastic bed, the velocities u and v are instead given in terms of the potential Φ and the shear function Ψ as

$$u = \frac{\partial \Phi}{\partial x} + \frac{\partial \Psi}{\partial y}, \quad v = \frac{\partial \Phi}{\partial y} - \frac{\partial \Psi}{\partial x} \tag{7}$$

where Φ is still governed by Laplace's equation (5), while Ψ is governed by the elastic shear-wave equation

$$c_s^2 \nabla^2 \Psi = \frac{\partial^2 \Psi}{\partial t^2}, \quad c_s = (G/\rho)^{\frac{1}{2}}, \tag{8}$$

where c_s is the elastic shear-wave speed. The appropriate boundary conditions for the elastic solution should be to satisfy the conditions of continuity of pressure and normal velocity across the mudline. The continuity of shear stress and tangential

velocity across the interface will be satisfied separately by the boundary-layer solution at the mudline.

Thus, for the elastic solution below the mudline, it is seen from (4) and (7) that the continuity of the vertical velocity v requires that the potential Φ must have a discontinuity across the mudline. The other condition of continuity of normal stress across the interface furthermore requires that

$$\left(\rho\frac{\partial^2\Phi}{\partial t^2}\right)^+ = \left(2G\frac{\partial v}{\partial y}+\rho\frac{\partial^2\Phi}{\partial t^2}\right)^-, \tag{9}$$

where the superscripts + and − mean, respectively, just above and below the interface. By a simple dimensional argument, it is seen from (9) and (3) that the jump, or the discontinuity in Φ is of $O(\epsilon^2)$, i.e.

$$(\Phi^+-\Phi^-)/\Phi \sim O(\epsilon^2) \ll 1, \tag{10}$$

and this also should be the relative order of magnitude of the shear function Ψ (i.e. from the velocity continuity requirement)

$$\Psi/\Phi \sim O(\epsilon^2). \tag{11}$$

Following a standard perturbation scheme, the potential Φ in the whole water–bed domain $h > y > -\infty$ is expanded as

$$\Phi = \phi^{(0)}+\epsilon\phi^{(1)}+\epsilon^2\phi^{(2)}+\ldots, \tag{12}$$

where from (10) it appears that we need to carry the analysis to $\phi^{(2)}$ in order to account for the mudline elasticity. To be consistent, only the leading-order 'linear' solution for Ψ will be sought (cf. (11)) for $y < 0$. In order to allow for slow modulation in the wave, we introduce the following multiple scalings:

$$x, \quad x_1 = \epsilon x, \ldots, \quad t, \quad t_1 = \epsilon t, \quad t_2 = \epsilon^2 t, \ldots, \tag{13}$$

and assume $\phi^{(n)}$ to be functions of the above scales. Substituting (12) into (5), (6) and (9) we get a series of linear problems

$$\left(\frac{\partial^2}{\partial x^2}+\frac{\partial^2}{\partial y^2}\right)\phi^{(n)} = F^{(n)} \quad h \geqslant y > -\infty \tag{14}$$

with free-surface condition

$$\left(\frac{\partial^2}{\partial t^2}+g\frac{\partial}{\partial y}\right)\phi^{(n)} = H^{(n)} \quad \text{at} \quad y = h, \tag{15}$$

and at the interface, for $n > 1$

$$\frac{\partial^2}{\partial t^2}[(\phi^{(n)})^+-(\phi^{(n)})^-] = \left(\frac{2G_0}{\rho_0}\frac{\partial v}{\partial y}\right)^-, \tag{16}$$

and at large depth

$$\phi^{(n)} \to 0 \quad \text{as} \quad y \to -\infty. \tag{17}$$

The inhomogeneous terms $F^{(n)}$, $H^{(n)}$ are functions of the lower-order potentials $\phi^{(n-1)}$, $\phi^{(n-2)}, \ldots$, and the series is to be solved in sequence. It is clear that the solutions for

the first two potentials $\phi^{(0)}$ and $\phi^{(1)}$ are identical to those obtained for deep-water waves in homogeneous fluid, since there is no contribution from (16),

$$\left.\begin{aligned}\phi^{(0)} &= -\frac{igA}{2\omega}\,e^{k(y-h)}\,e^{i(kx-\omega t)}+*,\\ \phi^{(1)} &= 0.\end{aligned}\right\} \tag{18}$$

$\phi^{(0)}$ is the homogeneous wave solution ($F^{(0)} = H^{(0)} = 0$), and A is the wave amplitude, k is the wavenumber, and ω is the wave frequency

$$\omega^2 = gk, \tag{19}$$

and we assume the relation with the mudline elastic wavenumber, s_0 as in (3), i.e.

$$k = \mu s_0. \tag{20}$$

Now, for $\phi^{(2)}$, we may linearly decompose the solution by writing

$$\phi^{(2)} = \phi_h^{(2)} + \phi_e^{(2)}, \tag{21}$$

where $\phi_h^{(2)}$, like $\phi^{(0)}$ and $\phi^{(1)}$, is the classical solution for homogeneous fluid, while $\phi_e^{(2)}$ is the new elastic, discontinuous solution. We require $\phi_h^{(2)}$ to satisfy (14), (15) and (17) which are identical to the conditions for the third-order potential for deep-water waves (see e.g. Mei 1983). In particular, the solvability condition for $\phi_h^{(2)}$ will yield the familiar evolution equation for the wave amplitude A in the form of a nonlinear Schrödinger equation (Zakharov 1968)

$$\left(\frac{\partial}{\partial t_1}+c_g\frac{\partial}{\partial x_1}\right)A = -i\epsilon\left\{\frac{\omega}{8k^2}\frac{\partial^2 A}{\partial x_1^2}+\tfrac{1}{2}\omega k|A|^2 A\right\}, \tag{22}$$

where $c_g = g/2\omega$ is the group velocity of deep water.

On the other hand, $\phi_e^{(2)}$ satisfies (14) and (15) with zero right-hand sides, along with (16) and (17). The role of $\phi_e^{(2)}$ is then to slightly modify the dispersion relation (19). When combining $\phi_e^{(2)}$, which is discontinuous at the mudline, with the viscous boundary-layer solution at the mudline, the modification to k in (19) becomes complex, with the imaginary k corresponding to the associated damping of the carrier wave.

Besides the direct damping of the carrier wave energy by viscous friction at the mudline, there also exists the possibility of a sideband instability through which the carrier wave would lose some of its energy to a narrow band of sideband oscillations. This well-known result, due to Benjamin & Feir (1967), can be seen by slightly perturbing the Stokes wave solution to (22) with large-scale modulations, i.e. we let

$$A = (A_0 + a\exp[i(Kx_1'-\Omega t_2)\exp[-\tfrac{1}{2}i\omega k^2|A_0|^2 t_2)]; \quad x_1' = x_1 - c_g t_1, \tag{23}$$

where A_0 is the amplitude of the nonlinear Stokes wave, and a is the amplitude of the small perturbation over the long modulational scales of x_1' and t_2. Substituting (23) into (21) and dropping nonlinear terms in a, we see that Ω becomes pure imaginary (i.e. linear instability) in the narrow sideband

$$|K/k| < \sqrt{8kA_0}. \tag{24a}$$

The maximum energy transfer occurs when $|K/k| = 2kA_0$, at which

$$\text{Max}\,\Omega = \pm i\tfrac{1}{2}\omega(k^2 A_0^2). \tag{24b}$$

The question of interest here is to investigate the fate of this transferred energy to the sideband perturbations in the presence of the small mudline elasticity and viscosity. This would clearly depend on the modification of the dispersion relation by $\phi_e^{(2)}$ and Ψ, and is investigated in the following section.

3. The eigenvalue problem

Since both $\phi^{(0)}$ and $\phi_e^{(2)}$ satisfy the same governing equations, except condition (16), it is convenient here to superimpose the two potentials and solve for the combined response, i.e. we write

$$\phi = \phi^{(0)} + \phi_e^{(2)}, \tag{25}$$

where from (14)–(17) we see that ϕ satisfies

$$\left(\frac{\partial^2}{\partial x^2} + \frac{\partial^2}{\partial y^2}\right)\phi = 0, \tag{26}$$

$$\left(\frac{\partial^2}{\partial t^2} + g\frac{\partial}{\partial y}\right)\phi = 0 \qquad \text{at} \quad y = h, \tag{27}$$

$$\frac{\partial^2}{\partial t^2}(\phi^+ - \phi^-) = \left(\frac{2G_0}{\rho_0}\frac{\partial v}{\partial y}\right)^- \quad \text{at} \quad y = 0, \tag{28}$$

$$\phi \to 0 \qquad \text{as} \quad y \to -\infty. \tag{29}$$

Furthermore, the requirement of continuity of vertical velocity across the mudline implies from (4) and (7) that

$$\frac{\partial}{\partial y}(\phi^+ - \phi^-) = -\frac{\partial \Psi}{\partial x} \quad \text{at} \quad y = 0, \tag{30}$$

with Ψ satisfying (8). The mudline boundary layer satisfies the remaining continuity conditions on shear stress and horizontal velocity. In the boundary layer, the total velocity u is composed of the inviscid velocity $\nabla\phi$, plus a rotational velocity $\boldsymbol{U} = (U, V)$. The governing boundary-layer equation for U is

$$\frac{\partial U}{\partial t} = \nu\frac{\partial^2 U}{\partial y^2} \tag{31}$$

with the boundary conditions

$$U \to 0 \quad \text{as} \quad y/\delta \to \infty \quad \text{(outside the boundary layer)}, \tag{32}$$

$$\frac{\partial}{\partial x}(\phi^+ - \phi^-) = \frac{\partial \Psi}{\partial y} - U \qquad \text{at} \quad y = 0, \tag{33}$$

$$\frac{\partial}{\partial t}\tau_0 = \frac{\partial}{\partial t}\left(\rho_0 \nu \frac{\partial U}{\partial y}\right) = G_0\left(\frac{\partial u}{\partial y} + \frac{\partial v}{\partial x}\right)^- \quad \text{at} \quad y = 0, \tag{34}$$

where (33) is the condition for continuity of horizontal velocity, and (34) is the condition for continuity of shear stress.

3.1. *The potential* ϕ

The solution to (26) in the inviscid water layer is given by

$$\phi = (a\,e^{ky} + b\,e^{-ky})\,e^{i(kx-\omega t)} \quad h > y > 0, \tag{35}$$

where from (27) and (30) we have

$$a = b + \frac{v_0}{k} \tag{36}$$

and

$$b = \frac{v_0}{2k}\,\frac{(kg/\omega^2 - 1)\,(\tanh kh + 1)}{1 - (kg/\omega^2)\tanh kh}, \tag{37}$$

and where v_0 is the amplitude of the mudline vertical velocity. Below the mudline, the solution to (27) is instead given by

$$\phi = c\,e^{ky}\,e^{i(kx-\omega t)} \quad y < 0, \tag{38}$$

where the amplitude c is to be found by solving for the elastic response in the bed. Notice that in the absence of bed elasticity, k and ω would exactly satisfy the deep-water dispersion relation (19), which means that b would vanish and ϕ would be continuous throughout.

3.2. *The elastic shear wave in the stratified bed*

A WKB solution to (8) for the shear function Ψ is given by (see e.g. Aki & Richards 1980)

$$\Psi = \left\{\frac{a'}{(s^2-k^2)^{\frac{1}{4}}}\exp\left[i\int_{y_p}^{y}(s^2-k^2)^{\frac{1}{2}}dy\right] + \frac{b'}{(s^2-k^2)^{\frac{1}{4}}}\exp\left[-i\int_{y_p}^{y}(s^2-k^2)^{\frac{1}{2}}dy\right]\right\}e^{i(kx-\omega t)}, \tag{39a}$$

where

$$s = \omega/c_s = (\rho\omega^2/G)^{\frac{1}{2}} \tag{39b}$$

is the shear wavenumber, which is assumed to change slowly with depth, a' and b' are constants, and y_p is the depth of the turning point at which the shear wavenumber becomes equal to the water-wave wavenumber, i.e.

$$s = k \quad \text{at} \quad y = y_p. \tag{40}$$

Above the turning point, the solution for Ψ is oscillatory, made out of two shear waves, one moving upward and one moving downward. Below the turning point, the solution is exponential and is required to decay to infinity. Through standard turning-point manipulation, the oscillatory and the exponentially decaying solutions may be matched via Airy's function, yielding a condition on the constants a' and b', namely

$$a' = E\,e^{-i\pi/4}, \quad b' = E\,e^{i\pi/4}, \tag{41}$$

where E is a constant. Near the mudline, where $G = G_0$ and $\rho = \rho_0$, we may approximate (39a) as

$$\Psi = F\cos(s_0 my + \beta)\,e^{i(kx-\omega t)} \quad \text{near} \quad y = 0, \tag{42a}$$

where

$$m = (1-\mu^2)^{\frac{1}{2}}, \tag{42b}$$

$$\beta = \int_{y_p}^{0}(s^2-k^2)^{\frac{1}{2}}dy - \tfrac{1}{4}\pi \tag{42c}$$

and F is a constant.

3.3. *The viscous flow in the boundary layer*

The solution to (31) that satisfies (32) is given by

$$U = U_0 \exp\left[(-1+\mathrm{i})\left(\frac{\omega}{2\nu}\right)^{\frac{1}{2}} y\right] \mathrm{e}^{\mathrm{i}(kx-\omega t)}, \tag{43}$$

where from (33) we get an expression for U_0:

$$U_0 = -Fs_0 m \sin\beta - \mathrm{i}k(a+b-c), \tag{44}$$

and from (34) we get the expression for the mudline shear: $\tau_0 = \hat{\tau}_0 \mathrm{e}^{\mathrm{i}(kx-\omega t)}$, with the amplitude $\hat{\tau}_0$ given by

$$-\mathrm{i}\omega\hat{\tau}_0 = (1+\mathrm{i})\rho_0\omega(\nu\omega/2)^{\frac{1}{2}} U_0 = G_0[2\mathrm{i}k^2 c + (2k^2 - s_0^2) F\cos\beta]. \tag{45}$$

3.4. *The dispersion relation*

From (28), (30), (33) and (34) we get the non-dimensional amplitudes of the velocity functions ϕ and Ψ in the bed, i.e.

$$\frac{\phi^-}{\phi^+} = \frac{c}{a+b} = \frac{(1-2\mu^2) - 2\mu m \tan\beta T}{(1-2\mu^2)^2 + 4\mu^3 \tan\beta}, \tag{46}$$

$$\frac{F}{\phi^+} = \frac{\mathrm{i}\mu^2 - 0.5(1-2\mu^2)\, T}{(1-2\mu^2)^2 \cos\beta + 4\mu^3 m \sin\beta}, \tag{47}$$

where
$$T = \frac{\hat{\tau}_0}{\rho_0\omega\phi^+} = \frac{1+\mathrm{i}}{\sqrt{2}}(s_0\delta)\left[\mu + \frac{\mu(2\mu^2-1) + 2\mu^2 m\tan\beta}{(1-2\mu^2)^2 + 4\mu^3 m\tan\beta}\right](1+O(s_0\delta)), \tag{48a}$$

with
$$s_0\delta = \left(\frac{\nu\omega}{G_0/\rho_0}\right)^{\frac{1}{2}} \ll 1. \tag{48b}$$

From (7) we get an expression for the non-dimensional amplitude v_0 of the mudline vertical velocity:

$$\frac{v_0}{k\phi^+} = \frac{1}{(1-2\mu^2)^2\cos\beta + 4\mu^3 m\sin\beta}(1+O(T)). \tag{49}$$

Finally, we may relate the amplitude $\phi^+ = a+b$ to the wave amplitude A at the water surface through the linear kinematic boundary condition

$$\frac{\partial\phi}{\partial y} = \frac{\partial}{\partial t}(A\,\mathrm{e}^{\mathrm{i}(kx-\omega t)}) \quad \text{at} \quad y = h \tag{50}$$

which, from (35) and (49), yields

$$\phi^+ = \frac{-\mathrm{i}gA}{2\omega\cosh(kh)}\left[1 + \frac{\tanh(kh)}{(1-2\mu^2)^2 + 4\mu^3 m\tan\beta}\right]^{-1}. \tag{51}$$

On the other hand, the linear dispersion relation may be obtained by substituting (36) and (37) into (49) to get the relation for the non-dimensional wavenumber $\mu = k/s_0$

$$[(1-2\mu^2)^2 + 4\mu^3 m\tan\beta - 1][1 - \lambda\mu\tanh\mu h'] = (\lambda\mu - 1)(\tanh\mu h' + 1)(1+O(T)), \tag{52a}$$

where
$$\lambda = s_0 g/\omega^2, \quad h' = s_0 h. \tag{52b, c}$$

Strictly speaking, the above dispersion relation is to be solved coupled with the integral equation (42c) for β, to get a discrete set of the possible eigenvalues. However, as the turning point y_p gets deeper below the mudline, the number of possible eigenvalues would increase in the range $0 < \mu < 1$ until we approach the condition of an almost continuous μ-spectrum for very deep turning point (i.e. very large β). In this case, μ can assume almost any value between zero and 1, and (52a) would merely serve to determine the corresponding β-value (to a $2\pi n$ additive).

Out of this almost continuous spectrum of eigenvalues, our main interest here is primarily focused on what happens in a narrow band around the true surface wave solution near the linear wavenumber (19). In particular, we are interested in the wave damping characteristics at and near the surface wave eigenvalue. The dissipation of wave energy is assumed to take place in the mudline boundary layer and is given by (e.g. Dalrymple & Liu 1978)

$$P_d = \rho_0 \nu \int_0^\infty \overline{\left(\frac{\partial U}{\partial y}\right)^2} \, dy, \tag{53}$$

where the overbar denotes the time average over one wave period, and P_d is the rate of energy dissipation per unit surface area. Thus, a steady-state wave energy balance requires

$$c_g \frac{\partial E_w}{\partial x} = -P_d, \tag{54}$$

where E_w is the wave energy density

$$E_w = \tfrac{1}{2}\rho_0 g |A|^2. \tag{55}$$

From (43) and (45) we see that energy dissipation is given by

$$P_d = |\hat{\tau}_0|^2 / 2\rho_0 (\omega\nu)^{\frac{1}{2}}, \tag{56}$$

where the mudline shear amplitude $\hat{\tau}_0$ is given by (48a) and (51). Thus, in terms of a linear wave damping rate k_i (i.e. the imaginary part of the eigenvalue), which we see from (54) is given by

$$k_i = P_d / (2 c_g E_w). \tag{57}$$

Figure 2 shows sample results for the calculated damping rate k_i in a narrow band around the surface-wave wavenumber $\sim \omega^2/g$ and for a range of mudline shear-wave speeds $c_s(0) = (G_0/\rho_0)^{\frac{1}{2}}$ and a selected mudline viscosity $\nu = 10^{-5}$ m^2/s, a water-layer depth of 5 m, and wave period $T = 10$ s. Each curve in the figure gives the non-dimensional wavenumber kg/ω^2 as a function of $c_s(0)$ for a fixed damping rate k_i. A true surface wave is thus defined here as the one that experiences zero damping, i.e. is represented by the curve $k_i = 0$ in the figure. This zero damping would occur if the mudline boundary layer vanishes, that is when there is a perfect match in tangential velocities of the inviscid water layer and the elastic bed at the mudline. It is seen from the figure that such a surface wave occurs for k slightly lower than the inviscid deep-water wavenumber ω^2/g (non-dimensional wavenumber slightly lower than unity).

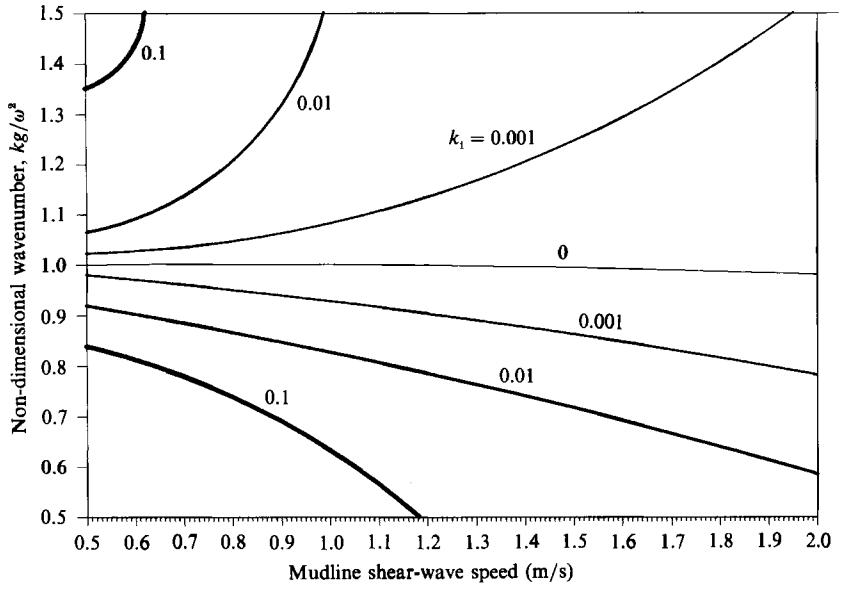

FIGURE 2. Non-dimensional wavenumber kg/ω^2 as a function of the mudline shear-wave speed $c_s(0) = (G_0/\rho_0)^{\frac{1}{2}}$ for various values of wave damping rate k_i.

4. Discussion of results

The most important feature of the results in figure 2 is the relatively strong damping associated with the sideband oscillations around the true surface-water solution. This is particularly the case for very small mudline shear-wave speed, where a less than 1% deviation in wavenumber from the zero-damping 'true surface wave' solution would result in a very large jump in damping rate to $k_i > 0.1$ m^{-1}, i.e. an almost critically damped wave. This can be seen directly from the obtained results by first considering the dispersion relation (52a). For the surface wave solution, we have

$$\mu \approx \lambda^{-1} \tag{58a}$$

which means, by balancing both sides of (52a), that

$$\tan\beta \approx O(\mu^{-1}) \quad \text{for a surface wave.} \tag{58b}$$

Now, from (24a), we see that the unstable sideband perturbation in wavenumber is of $O(\epsilon)$ where ϵ is the wave steepness. Thus, if instead of (58a) we let

$$\mu \approx \lambda^{-1}(1+\epsilon) \tag{59a}$$

we get from (52a) and (3a) that

$$\tan\beta \approx O(\mu^{-2}) \quad \text{for sidebands.} \tag{59b}$$

We then substitute the above orders of magnitude into (57) to get the associated changes in the damping rate. From (51), it is seen that there is hardly any change in ϕ^+ (i.e. the mudline pressure) over the range from (58) to (59). However, there is a significant change in T, or the mudline shear over the same range. This is seen from (48) which gives $T \sim O(k\delta)$ if we assume the surface-wave scaling (58), increasing significantly to $T \sim O(s_0\delta)$ by assuming the sideband scaling (59). This is an increase of $O(\mu^{-1})$ over the narrow span of the unstable sideband. The reason is primarily

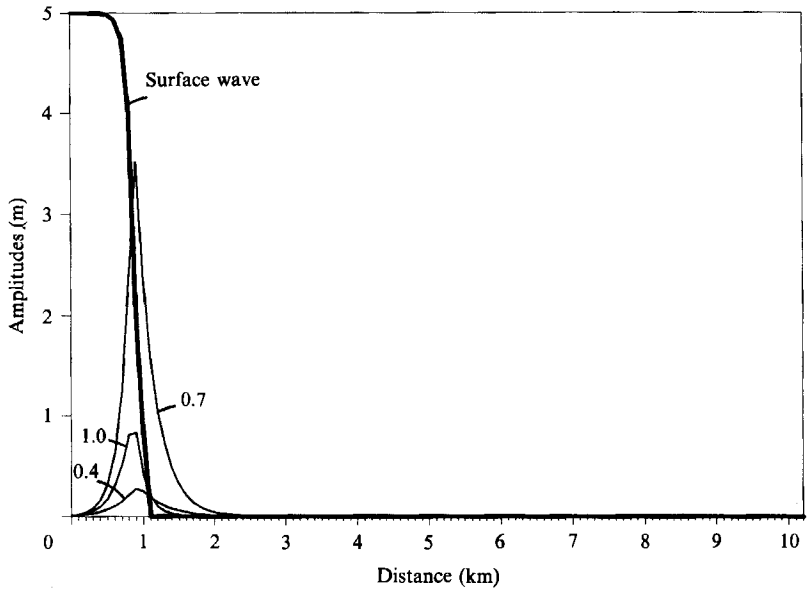

FIGURE 3. Sideband damping of a 5 m–10 s surface wave by three upper sidebands with modulational wavenumbers $K = (1, 0.7, 0.4)\, 2k_0^2 A_0$. The deep bottom mud has a mudline shear-wave speed = 1 m/s.

attributed to the role of the short shear waves in the elastic bed as they interact with the viscous mudline boundary layer. Although the relative amplitude of the shear wave is proportional to $O(\mu^2) \ll 1$, its lengthscale relative to the gravity wave is of $O(\mu)$ so that it produces large gradients and hence $O(1)$ shear stress at the mudline (cf. (45)). The exception occurs for surface wave solutions where the total shear stress at the mudline vanishes or almost vanishes identically due to the matching of the non-viscous tangential velocities there, i.e. the $k_i \approx 0$ condition.

For an illustration, we calculate the linear evolutions of three sideband perturbations to a surface wave of amplitude 5 m and period 10 s over a deep mud bank with $c_s(0) = 1$ m/s (figure 3). Each sideband has a different modulational wavenumber $K = (1, 0.7, 0.4) K_{max}$, where K_{max} is the modulation $K_{max} = 2k_0^2 A_0$ for the maximum energy transfer as given in (24*b*). The initial amplitude of each sideband at $x = 0$ was set at 0.01 m. The linear spatial growth rate for any unstable sideband is given by (Benjamin & Feir 1967)

$$\alpha = \frac{\omega}{c_g} \left\{ \frac{K^2}{8k_o^2} \left(k_0^2 A_0^2 - \frac{K^2}{8k_0^2} \right) \right\}^{\frac{1}{2}}, \tag{60}$$

where k_0 is the linear wavenumber ω^2/g. The sideband perturbations will be subjected to this linear growth rate, as well as the linear viscous decay rate k_i from figure 2. The calculation was made for each sideband by assuming that, locally, the carrier-wave amplitude A_0 is uniform so that we can use (60). Then, the net growth rate would be the difference $\alpha - k_i$ for each sideband. As we progress one step in distance x in the direction of wave propagation, we calculate the change in A_0 from the energy-balance equation (54), where now the energy E_w is the total energy of all the waves, and P_d is the energy loss from the three sidebands. Figure 3 shows the obtained profiles. A spectacular damping of the wave energy is quite evident from the figure. Recall

that the kinematic viscosity in the boundary layer is assumed to be only 10^{-5} m^2/s, or only ten times that of pure water. For comparison, all other linear models would produce a damping lengthscale of about 10 km or longer if using the same kinematic viscosity (e.g. Dalrymple & Liu 1978; MacPherson 1980). As discussed before, wave energy is first transferred to the sideband perturbations causing them to grow. Notice that the modulation receiving the maximum sideband growth rate, $K = K_{max}$, did not grow to be the largest sideband. This is because its damping rate k_i was also the largest among the sidebands. Therefore, there is an optimum modulational wavenumber, slightly less than K_{max}, that will draw most of the energy from the carrier wave before losing it quickly to boundary-layer friction. In figure 3, this corresponds to the $K = 0.7K_{max}$ sideband. We further observe that all the generated sidebands are very short-lived because of their high damping rates. Repeating the calculations for different wave frequency, we obtained less spectacular damping rates for longer waves and more spectacular damping for shorter ones. But in all cases they are orders of magnitude higher than the rate due to direct viscous damping which is proportional to $(\omega\nu)^{\frac{1}{2}}$.

Although the analysis predicts the trend to continue as $G_0 \to 0$, a practical lower limit on this mechanism would be due to the breakdown of the elasticity assumption for very small mudline shear modulus G_0. In reality, for very small G_0, a yield condition would be reached for large enough wave-induced shear forcing. This would result in the 'fluidization' of part of the soft bed, and thus the effective *lowering* of the mudline interface between the fluid layer and the elastic 'non-fluidized' bed with now *larger* G_0. After such 'plastic' adjustment of the sea–seabed system, the present model would still be applicable to describe the subsequent interaction.

This research was supported by grants from the National Science Foundation (MSM-8718951) and the University of California Water Resources Center (W-702).

REFERENCES

AKI, K. & RICHARDS, P. G. 1980 *Quantitative Seismology: Theory and Methods*. San Francisco: Freeman.

BEA, R. G. 1974 In *Proc. 6th Offshore Tech. Conf. OTC* 2110, pp. 791–810.

BENJAMIN, T. B. & FEIR, J. E. 1967 *J. Fluid Mech.* **27**, 417–430.

DALRYMPLE, R. A. & LIU, P. L.-F. 1978 *J. Phys. Oceanogr.* **8**, 1121–1131.

GADE, H. G. 1958 *J. Mar. Res.* **16**, 61–82.

HSIOH, S. V. & SHEMDIN, O. H. 1980 *J. Phys. Oceanogr.* **10**, 605–610.

JACOB, P. G. & QASIM, S. Z. 1974 *Indian J. Mar. Sci.* **3**, 115–119.

MACPHERSON, H. 1980 *J. Fluid Mech.* **79**, 721–742.

MEI, C. C. 1983 *Applied Dynamics of Ocean Surface Waves*, p. 616. Wiley.

PUTNAM, J. A. 1949 *Trans. Am. Geophys. Un.* **30**, 349–356.

WELLS, J. T. 1983 *Can. J. Fisheries Aquat. Sci.* **40**, 130–142.

ZAKHAROV, V. E. 1968 *J. Appl. Mech. Tech. Phys.* **2**, 190–194.